CrystEngComm

Complex Cobalt Silicates and Germanates Crystallizing in a Porous Three-Dimensional Framework Structure

Journal:	*CrystEngComm*
Manuscript ID	CE-ART-10-2019-001662.R1
Article Type:	Paper
Date Submitted by the Author:	15-Dec-2019
Complete List of Authors:	Usman, Mohammad; University of South Carolina, Chemistry and Biochemistry Smith, Mark; University of South Carolina, Department of Chemistry and Biochemistry Kocevski, Vancho; University of South Carolina, Mechanical Engineering Besmann, Theodore; University of South Carolina, Mechanical Engineering Zur Loye, Hans-Conrad; University of South Carolina, Department of Chemistry and Biochemistry

Complex Cobalt Silicates and Germanates Crystallizing in a Porous Three-Dimensional Framework Structure

Mohammad Usman,[1] Mark D. Smith,[1] Vancho Kocevski,[2#] Theodore Besmann,[2] and Hans-Conrad zur Loye, [1*]

[1]*Department of Chemistry and Biochemistry, University of South Carolina, Columbia, SC 29208, United States*

[2]*Department of Mechanical Engineering, University of South Carolina, Columbia, South Carolina 29208, United States*

Abstract: Four new cesium containing complex cobalt oxides, $Cs(Co_{0.5}Si_{0.5})SiO_4$ (**1**), $Cs_{1.29(5)}Co_{0.69(5)}Ge_{1.81(5)}O_5$ (**2**) and its ordered analogue $Cs_2CoGe_4O_{10}$ (**3**), were synthesized using a mixed CsCl-CsF flux at 850 °C and 900 °C, respectively. The structure of (**1**) closely resembles that of known zeolite and feldspar structure types and crystallizes in the noncentrosymmetric monoclinic space group *Im* with lattice parameters of a = 8.9926(4) Å, b = 5.4599(2) Å, c = 9.3958(6) Å and β = 91.5928(18)°. Structures (**2**) and (**3**) crystallize in the same new structure type, a highly porous three-dimensional framework, in the tetragonal space group *I*-4 with lattice parameters of a = 7.4239(14) Å and c = 13.169(3) Å and a = 7.3540(6) Å and c = 13.1122(11) Å, respectively. The formation of (**2**) vs (**3**) can be targeted by using slight variations in the quantities of starting materials. Single crystal to single crystal ion exchange experiment on (**1**) carried out in a molten $RbNO_3$ bath results in 14% Cs exchange with Rb, affording the composition, $Cs_{0.86}Rb_{0.14}(Co_{0.5}Si_{0.5})SiO_4$ (**4**). First-principles calculations in the form of density functional theory (DFT) were performed for (**1**) and (**3**) to elucidate their electronic and magnetic properties, and stability at 0 K.

Keywords: Flux growth, Cobalt oxides, Ion exchange, DFT calculations

**Corresponding Author's Email: zurloye@mailbox.sc.edu*

- current address: MST-8, Los Alamos National Laboratory, Los Alamos, NM 87545, USA

1. Introduction

Quaternary alkali cobalt silicates and germanates are rather scarce and most that are reported were structurally characterized from powder X-ray diffraction data.[1-4] Among the silicates, only three quaternary Cs/Co/Si/O phases have been deposited in the ICSD database; specifically, Cs_2CoSiO_4, Cs_5CoSiO_6 and $Cs_2CoSi_5O_{12}$.[4,5] In these mixed cobalt silicates, the substantial size difference between Co^{3+} (r = 0.545 Å – low spin octahedral coordination) and Si^{4+} (r = 0.26 Å - tetrahedral coordination) should ensure that no site mixing occurs between cobalt and silicon; surprisingly, Co^{3+}/Si^{4+} site-mixing is nonetheless observed in Cs_5CoSiO_6, which features two Co/Si mixed-metal sites. In contrast, typically, no site mixing is observed in Co^{2+} containing silicates. For example, Cs_2CoSiO_4 features ordered Co and Si sites. This may reasonably be attributed to the larger ionic size of Co^{2+} (r = 0.58 Å – high spin tetrahedral coordination), in addition to the larger charge difference between the +2 Co and +4 Si. In this work, we introduce another example, Co(II) containing $Cs_2CoSi_3O_8$, which features both, two unique silicon sites and two mixed Co(II)/Si sites.

Interest in this class of materials arises from the ablity to prepare members of this family of silicates in non-centrosymmetric structures, which makes such materials potentially SHG active and hence of interest for applications based on non-linear optical properties. To date, no reported quaternary Cs/Co/Ge/O systems have been structurally characterized by single crystal X-ray diffraction, although a number of ternary cobalt germanates have been observed, including $CoGeO_3$, $Co_{10}Ge_3O_{16}$, and Co_2GeO_4.[6-8] Hence, the ability to obtain these phases in single crystal form is highly desirable as it can greatly improve their structural characterization (vide infra). During crystal growth, it is generally accepted that an ordered vs. disordered structure, in this case the presence or absence of Co/Ge site mixing, is influenced by the thermodynamic stability of different site occupancies, as well as by the speed of crystal formation. Representative examples of this are two of the phases discussed in this paper, $Cs_{1.29(5)}Co_{0.69(5)}Ge_{1.81(5)}O_5$ (**2**) and its ordered analogue $Cs_2CoGe_4O_{10}$ (**3**), which are isostructural but differ in the presence and absence of Co/Ge site mixing.

We successfully explored the molten cesium halide flux crystal growth and prepared three new, complex cobalt silicates and germanates. Herein we report the synthesis of (**1**) – (**3**), DFT calculations, and the formation of the ion exchange product of (**1**), $Cs_{0.86}Rb_{0.14}(Co_{0.5}Si_{0.5})SiO_4$ (**4**).

2. Experimental section

2.1. Reagents

CoF_2 (Alfa Aesar, anhydrous powder, 98%), SiO_2 (Alfa Aesar, 99.9%), GeO_2 (99.999%, Alfa Aesar), RbCl (Alfa Aesar, 99.8%), RbF (99.1%, Alfa Aesar), $RbNO_3$ (Alfa Aesar, 99.8%), CsCl (Ultra-pure, VWR) and CsF (Alfa Aesar, 99.9%) were used as received without any further modification for the synthesis of all title compounds.

2.2. Flux Growth

Single crystals of the title compounds were obtained via mixed CsCl-CsF flux growth. In general, these compounds were synthesized by charging a 7.5 cm tall by 1.2 cm diameter cylindrical silver crucible, with one of its ends sealed and welded shut using a TIG-175 Square Wave Lincoln Electric welder, with CoF_2, TO_2 (T = Si, Ge), and the appropriate amount of CsCl-CsF flux. The specific amounts of the reagents and the flux, in addition to the heating and cooling cycle, are listed in Table 1. The tube containing the charge was placed into a programmable furnace and heated to the reaction temperature, held at this temperature for the desired number of hours, and then slow cooled to well below the melting point of the flux, whereupon the furnace was shut off. In all three cases, deep blue crystals with different morphologies were obtained by dissolving the solidified flux in warm distilled water, aided by sonication, and washing the crystals with acetone during vacuum filtration. Typical yield was less than 25%.

2.3. Energy-Dispersive Spectroscopy

Elemental analysis was performed on single crystals of all compounds using a TESCAN Vega-3 SBU scanning electron microscope (SEM) with EDS capabilities. Single crystals of (**1**) – (**4**) were mounted on carbon tape and analyses was carried out using a 20-kV accelerating voltage and accumulation time of 20 s. EDS verified the presence of the appropriate elements in all compositions. The absence of extraneous elements in the product crystals, such as silver from the reaction vessel, was confirmed within the detection limits of the instrument. Semi-quantitative elemental analyses results are provided in the Supporting Information (SI).

2.4. Ion Exchange

Single crystal to single crystal ion exchange reactions were performed on (**1**) by layering 0.1 g of crystals of the sample under 1 g of $RbNO_3$ in a fused-silica ampoule measuring 7.5 cm in length. The tube containing the charge was heated at 350 °C for 16 h. Once the reaction was complete, the flux was dissolved in hot water and the crystals were thoroughly rinsed and examined by single crystal X-ray diffraction.

2.5. Single Crystal X-ray Diffraction

X-ray intensity data from suitable crystals of (**1**) – (**4**) were collected at 301(2) K using a Bruker D8 QUEST diffractometer equipped with a PHOTON 100 CMOS area detector and an Incoatec microfocus source (Mo Kα radiation, λ = 0.71073 Å).[9] The raw area detector data frames were reduced and corrected for absorption effects using the SAINT+ and SADABS programs.[9,10] Initial structural models were obtained with SHELXT.[11] Subsequent difference Fourier calculations and full-matrix least-squares refinement against F^2 were performed with SHELXL-2018 using the ShelXle interface for (**2**), (**3**), and OLEX2 for (**1**) and (**4**).[12,13] Crystallographic data, refinement data, and interatomic distances for all compounds are listed in Tables 2 – 6. A detailed crystallographic discussion is provided in the SI.

2.5. First-principles calculations

First-principles calculations were performed in the form of density functional theory (DFT) with an on-site Coulomb interaction, i.e., DFT+U, using the Vienna Ab-initio Package (VASP) code,[14,15] using the projector augmented wave (PAW) method,[16,17] and generalized gradient approximation of Perdew, Burke and Ernzerhof (PBE).[18] To model the Si/Co mixing and partial occupies of the Cs atom in (**1**) and (**3**), super quasi-random structures (SQSs) were made (relaxed SQSs are given in the SI). Structures (**2**) and (**4**) could not be reproduced because reproducing the low Co and Rb concentration requires a huge SQSs (> 1000 atoms), making the calculations prohibitively expensive. To see if (**1**) and (**3**) are thermodynamically stable, i.e., if they break the Cs-Co-Si-O and Cs-Co-Ge-O convex hulls, respectively, their formation energy was compared with respect to the Open Quantum Materials Database (OQMD).[19] We used the OQMD calculations set-up: 520 eV cut-off energy for the plane wave basis set, 10^{-4} eV energy convergence criterion, 6×9×5 and 7×7×4 **k**-point meshes for (**1**) and (**3**), respectively, and U_{eff} = 3.3 eV for the Co atoms. The system was considered to be spin-polarized, with high-spin ferromagnetic (FM) and antiferromagnetic (AFM) (0 μ_B magnetic moment) ordering of the Co atoms.[20] For calculating the electronic and optical properties, more rigorous calculations were performed, using 520 eV cut-off energy for the plane wave basis set, 10^{-6} eV and 10^{-3} eV/Å energy and forces convergence criteria, respectively, and the same **k**-point mesh as the OQMD calculations. The ground state geometry was obtained by relaxing the cell volume, cell shape and atomic positions. The adsorption indexes of (**1**) and (**3**) were obtained from the calculated frequency dependent dielectric function in the independent-particle picture.

3. Results and Discussion

3.1. Synthesis

Mixed alkali fluoride-chloride melts have been remarkably successful for crystallizing complex silicates and germanates[21] and were used to obtain single crystals of the title compounds, $Cs(Co_{0.5}Si_{0.5})SiO_4$ (**1**), $Cs_{1.29(5)}Co_{0.69(5)}Ge_{1.81(5)}O_5$ (**2**) and $Cs_2CoGe_4O_{10}$ (**3**). None of the crystal growth reactions described herein, however, yielded a phase-pure product and numerous attempts to obtain a phase-pure product by adjusting temperature, reagent ratios etc. failed. Due to the small size of the crystals, it was not possible to pick a phase-pure sample of any of the title compounds. In addition, attempts to synthesize (**1**) and (**3**) via a solid-state approach also did not result in a phase-pure product. In both cases, obtaining a pristine sample for physical property measurements was prevented by the formation of the undesired phases, $Cs_2CoSi_5O_{12}$ and $Cs_2CoGe_5O_{12}$. A solid-state synthesis of $Cs_2CoSi_5O_{12}$ was carried out to determine its magnetic properties, which have not been reported so far. The compound is a simple Curie paramagnet in the entire 2 – 375 K range with no obvious magnetic ordering down to 2 K.

It is quite fascinating to observe how different amounts of reagents subject to similar reactions conditions can lead to order and disorder in the same crystal structure. For instance, (**2**), which contains only mixed Co and Ge sites, can be prepared by layering 1 mmol of CoF_2 and 4 mmol of GeO_2 under 3.15 g of CsCl and 2.31 g of CsF. Decreasing the amount of GeO_2 to 2 mmol, and the amounts of CsCl and CsF to 1.85 g and 1.36 g, respectively, yields (**3**) which contains only ordered, fully occupied Co and Ge sites, and is isostructural to (**2**). In contrast, (**1**) can be synthesized by using either 1 mmol or 2 mmol of SiO_2; however, the crystal quality is worse when 2 mmol of SiO_2 are used. Further increases in the amount of SiO_2 leads to the formation of $Cs_2CoSi_5O_{12}$.[5] Similar reactions were also carried out using molten RbCl-RbF flux, which led to the formation of compounds displaying even higher structural complexity than the phases reported herein and will be reported elsewhere.

3.2. Crystal Structure and Ion Exchange

Structure (**1**) crystallizes in the monoclinic system in the space group *Im*. The asymmetric unit consists of two cesium atoms, two silicon atoms, two mixed sites modeled as 50/50 Co/Si and six unique oxygen atoms. The crystal structure of (**1**) is characteristic of the '1114' family of transition metal based lithium aluminosilicates.[22] Members of this family crystallize in a wide variety of space groups; $NaCoPO_4$ ($P6_1$), $KCoPO_4$ ($P6_3$), NH_4CoPO_4 ($P6_3$), $RbCoPO_4$ ($P2_1$) and

$TlZnAsO_4$ ($P2_1$).[23,24] The ABW[22] zeolite topology has been extensively studied previously and consists of six-ring sheets and zigzag chains.[25,26] Usually, the $ABTO_4$ type zeolites (A = alkali metal, B = divalent or trivalent metal, X = P, Si, or Ti) feature either ordered, alternating BO_4 and TO_4 tetrahedral frameworks, as observed in $CsFeSiO_4$, or a disordered framework, as observed in $CsAlTiO_4$, where the tetrahedral sites exhibit mixed Al/Ti occupancies.[26,27] $Cs(Co_{0.5}Si_{0.5})SiO_4$ (**1**) is a rare example, as can be seen from its structural formula, that features two unique Si sites as well as two mixed-metal sites that are 50/50 occupied by Co/Si. The crystal structure of (**1**) is comprised of corner-sharing Co(1)/Si(1A) and Co(2)/Si(2A) tetrahedral dimers bridged by the disordered O(5) that alternate with $Si(1)O_4$ and $Si(2)O_4$ pyrosilicate units via corner-sharing in a way that the resulting $(Co/Si)O_4$ and SiO_4 network features large eight-sided cavities running down the *b*-axis and relatively smaller, nearly perfect hexagonal (six-membered) channels running down the *a*-axis. These cavities and channels crisscross the crystal framework in all three directions and are occupied by fully ordered Cs cations that provide charge balance to the anionic cobaltosilicate framework. The Co(1)/Si(1A) to O and Co(2)/Si(2A) to O bond distances range from 1.821(16) Å – 2.012(11) Å and 1.405(10) Å – 1.781(17) Å, respectively. The unusually short Co to O distance of 1.405(10) Å can, at best, be attributed to the extensive disorder in the structure and is likely an artefact of the moderate crystallinity of the available sample. The Si-O bond lengths for $Si(1)O_4$ and $Si(2)O_4$ tetrahedra range from 1.550(10) Å – 1.680(12) Å and 1.592(11) Å – 1.670(11) Å, in good agreement with the typical value of ~1.64 Å for average Si-O bond lengths. Figure 1 illustrates the crystal structure of (**1**).

To determine if the Cs ions in the channels can be ion exchanged, single crystals of (**1**) were soaked in a molten $RbNO_3$ bath at 350 °C. The Cs ions undergo partial exchange and the product phase, $Cs_{0.86}Rb_{0.14}Co_{0.5}Si_{1.5}O_4$ (**4**), contains 14% Rb and 86% Cs, as determined by single crystal X-ray diffraction. The cobaltosilicate framework structure is unchanged by the ion exchange process. The presence of Rb in ion exchanged crystals was further corroborated by semi-quantitative EDS analysis.

The asymmetric unit of (**2**) consists of two unique mixed Co/Ge sites, Ge(1)/Co(1A) and Co(1)/Ge(1A), three unique oxygen atoms and a disordered distribution of electron density modeled as cesium atoms, most on general positions. The asymmetric unit of (**3**) consists of one Ge atom, one Co atom, three oxygen atoms and a disordered distribution of electron density modeled as cesium atoms, most on general positions, similar to (**2**). Structures (**2**) and (**3**) are

isostructural, and only differ in the degree of metal site mixing. For that reason, only the crystal structure of (**3**), which contains fully ordered Co and Ge sites, is described as following. (**3**) crystallizes in the tetragonal system in space group *I*-4. The crystal structure of (**3**) consists of a three-dimensional, porous network of corner sharing CoO_4 and GeO_4 tetrahedra that form large cavities occupied by severely disordered Cs cations that provide charge balance to the anionic cobaltogermanate framework. The three-dimensional framework consists of two-dimensional sheets of GeO_4 tetrahedra lying in the *ab*-plane. The GeO_4 tetrahedra corner-share exclusively forming dimers, with each dimer running along either the *a*- or *b*-axis, corner-sharing with four perpendicular dimers. This assembly of GeO_4 tetrahedra produces infinite two-dimensional sheets that are connected to each other via corner-sharing with CoO_4 tetrahedra along the *c*-axis. This structural arrangement is identical to the all-aluminate sheet topology that we recently reported for $Cs_2(UO_2)Al_2O_5$.[28] Each pair of alternating layers in (**3**) is connected by CoO_4 tetrahedra that corner-share with adjacent, facing up (UU) GeO_4 tetrahedra of the bottom layer and corner-share with adjacent, facing down (DD) GeO_4 tetrahedra of the top layer as illustrated in Figure 2. The Ge-O bond lengths in GeO_4 tetrahedra are 1.706(4) – 1.762(3) Å, whereas each CoO_4 tetrahedral unit is comprised of four equal bond lengths of 1.948 (4) Å. Figure 3 provides a perspective view of the crystal structure of (**3**).

It is interesting that under fairly similar reaction conditions (Table 1) two isostructural materials, (**2**) with and (**3**) without Co/Ge site mixing were obtained. The difference in the synthetic conditions lie solely in the relative amounts of reagents used. When starting with a 1:4 ratio of CoF_2/GeO_2, Co/Ge site mixing is obtained, while when starting with a 1:2 ratio of CoF_2/GeO_2, no Co/Ge site mixing is observed. One can speculate that the disordered phase (**2**) results from a fast crystal growth process that incorporates, at random, either Co or Ge onto the crystallographic site. In the case of (**3**), we can propose that the growth process is slower, enabling the selective filling of crystallographic sites by either all Co or all Ge. If we assume that the dissolution of GeO_2 is slow, then the presence of an increased amount of GeO_2 relative to CoF_2 can result in higher solution concentrations of Ge in a shorter amount of time, that ultimately leads to accelerated crystal growth. The size difference of Co(II) vs Ge(IV) should not lead to site mixing as both the size difference and the charge difference should favor unique crystallographic conditions – as observed for (**3**). As the heating rates and temperatures were identical, this leaves

the speed of crystal growth as one parameter that likely is responsible for the presence or absence of site mixing.

3.3. First-principles calculations

Compared to the experimental values for (**1**) and (**3**), the calculated lattice parameters of both FM and AFM systems are well reproduced by DFT, with an error < 3 % (see Table 7). Similarly, the total energy of the FM and AFM systems for both (**1**) and (**3**) are very close, with the FM having more negative energy by 1 meV/atom. Both (**1**) and (**3**) break the OQMD convex hull by 32 and 175 meV/atom, respectively, indicating that the formation of these compound is energetically favorable. Shown in Figure 4 are the projected density of states (DOS) of (**1**) in FM and AFM systems. It is evident that the FM DOS has two distinct band gaps in the spin up and spin down channels of 3.44 eV and 3.01 eV, respectively, while the AFM has only one band gap of 3 eV. The projected DOS (PDOS) show that the states around the band gap in (**1**) come predominantly from the Co atoms, signifying that $Cs(Co_{0.5}Si_{0.5})SiO_4$ compound is a Mott insulator, the same as CoO.[29] Similarly, the FM DOS of (**3**) has two band gaps of 2.52 and 2.07 eV in the spin-up and spin-down channels, and the AFM has only one band gap of 2.11 eV (Figure 5c). However, unlike (**1**), the states at the bottom of the conduction band of (**3**) come from the O atoms, while the states at the top of the valence band come from Co (Figure 5a and b), making $Cs_2CoGe_4O_{10}$ a charge-transfer insulator.

Following the similarity in the structure of (**1**) and (**3**), their DOS are also similar. Interestingly, the Co PDOS are almost at the same position in both (**1**) and (**3**), while the PDOS of the Ge and O are pushed closer to the band gap in (**3**). This push of the states towards the band gap comes from the higher energy of the Ge valence electrons ($4s^24p^2$) in (**3**), compared to the energy of the Si valence electrons ($3s^23p^2$) in (**1**). According to molecular orbital theory, the higher energy of the Ge valence electrons would give rise to Ge-O hybridized states at higher energy in the valence band, and lower energy in the conduction band, thus getting the Ge and O states closer to the band gap. Although, there is one more Ge atom in the (**3**) formula unit, $Cs_2CoGe_4O_{10}$, compared to Si atoms in the (**1**) formula unit, $Cs_2CoSi_3O_8$, this difference would have little influence on the position of the PDOS. Despite the different magnetic properties, the total DOS of the FM and AFM systems of (**1**) and (**3**) are very similar (Figure 4d and 5d), which gives rise to similar absorption indexes. On the other hand, the main difference between the adsorption indexes of (**1**) and (**3**) is the small peak at 3.4 eV in (**1**), which comes from the Co-Co transitions.

4. Conclusion

Using molten cesium halide flux crystal growth we have synthesized and structurally characterized one new cobalt containing cesium silicate, $Cs(Co_{0.5}Si_{0.5})SiO_4$ (**1**), and two new cobalt containing germanates, $Cs_{1.29(5)}Co_{0.69(5)}Ge_{1.81(5)}O_5$ (**2**) and $Cs_2CoGe_4O_{10}$ (**3**). The cesium ions in the cesium cobalt silicate can be partially ion exchanged for rubidium by soaking crystals in molten $RbNO_3$. All compounds crystallize in structure types featuring three-dimensional frameworks containing channels occupied by the monovalent alkali ions. Semi-quantitative elemental analyses confirmed the presence of all elements in the reported compositions. First-principles DFT calculations indicated that the formation of (**1**) and (**3**) is energetically favorable, where the FM state is slightly more stable than the AFM state in both compounds. The DOS indicate that (**1**) is a Mott insulator, similar to CoO, while (**3**) is a charge-transfer insulator.

Conflicts of Interest

There are no conflicts to declare.

Acknowledgements

M.U., M.D.S. and H.Z.L. performed the syntheses and structural characterization work and gratefully acknowledge the U.S. National Science Foundation for supporting this research through grant OIA-1655740. V.K. and T.M.B. acknowledge the support by the U.S. Department of Energy, Office of Science, Basic Energy Sciences, under Award No. DE-SC0016574 (Center for Hierarchical Waste Form Materials). This research used computational resources provided by the National Energy Research Scientific Computing Center (NERSC) and the HPC cluster Hyperion, supported by The Division of Information Technology at the University of South Carolina.

Supporting Information

An extended discussion of the crystallographic refinements for (**1**) – (**3**), single crystal optical images, and SEM and EDS results. CCDC 1905091 (**1**), 1905090 (**2**), 1957759 (**3**), and 1957758 (**4**) contain the supplementary crystallographic information for this paper. These data can be obtained free of charge via www.ccdc.cam.ac.uk/data_request/cif, or by emailing data_request@ccdc.cam.ac.uk, or by contacting The Cambridge Crystallographic Data Centre, 12 Union Road, Cambridge CB2 1EZ, UK; fax: +44 1223 336033.

Author Information

Mohammad Usman ORCID 0000-0002-9791-4364

Mark D. Smith ORCID 0000-0001-6977-7131

Vancho Kocevski ORCID 0000-0002-2127-5834

Theodore M. Besmann ORCID 0000-0002-6253-7693

Hans-Conrad zur Loye ORCID 0000-0001-7351-9098

References

1. H. Yamaguchi, K. Akatsuka, M. Setoguchi, and Y. Takaki, *Acta Crystallogr*., 1979, **35**, 2680.
2. W.A. Dollase, *Powder Diffraction*, 1996, **11**, 51.
3. G. Durand, S. Vilminot, M. Richard-Plouet, A. Derory, J.P. Lambour, and M. Drillon, *J. Solid State Chem*., 1997, **131**, 335-340.
4. J. Hansing, and A. Möller, *J. Solid State Chem*., 2001, **162**, 204-213.
5. A.M.T. Bell, and C.M.B. Henderson, *Acta Crystallogr. C*, 1996, **52**, 2132-2139.
6. D.R.Z. PEACOR, *Kristallogr*., 1968, **126**, 299-306.
7. J. Barbier, *Acta Crystallogr. C*, 1995, **51**, 343-345.
8. K. Hirota, M. Ohtani, N. Mochida, and A. Ohtsuka, *J. Ceram. Soc. Jpn*., 1989, **97**, 8-15.
9. **APEX3** Version 2016.5-0 and **SAINT+** Version 8.37A. Bruker AXS, Inc., Madison, Wisconsin, USA, 2016.
10. L. Krause, R. Herbst-Irmer, G.M. Sheldrick, and D. Stalke, *J. Appl. Cryst*., 2015, **48**, 3-10.
11. (a) G.M. Sheldrick, *Acta Cryst*. 2015, **A71**, 3-8. (b) G.M. Sheldrick, *Acta Cryst*., 2015, **C71**, 3-8.
12. C.B. Hübschle, G.M. Sheldrick, and B. Bittrich, *J. Appl. Cryst*., 2011, **44**, 1281-1284.
13. O.V. Dolomanov, L.J. Bourhis, R.J. Gildea, J. A. K. Howard, and H. Puschmann, *J. Appl. Cryst*., 2009, **42**, 339-341.
14. G. Kresse, and J. Furthmüller, *Phys. Rev. B*, 1996, **54**, 11169-11186.
15. G. Kresse, and J. Furthmüller, *Comput. Mater. Sci*., 1996, **6**, 15-50.
16. P.E. Blöchl, *Phys. Rev. B*, 1994, **50**, 17953-17979.
17. G. Kresse, D. and D. Joubert, *Phys. Rev. B*, 1999, **59**, 1758-1775.
18. J.P. Perdew, K. Burke, and M. Ernzerhof, *Phys. Rev. Lett*., 1996, **77**, 3865-3868.
19. J.E. Saal, S. Kirklin, M. Aykol, B. Meredig, and C. Wolverton, *JOM*, 2013, **65**, 1501-1509.
20. Low spin ferromagnetic ordering was also considered, but the calculations always converged to the high spin state.
21. D.E. Bugaris, and H.-C. zur Loye, *Angew. Chem. Int. Ed. Engl*., 2012, **51**, 3780-3811.
22. R.M. Barrer, and E.A.D. White, *J. Chem. Soc*., 1951, **283**, 1267-1278.
23. P. Feng, X. Bu, S.H. Tolbert, and G.D. Stucky, *J. Am. Chem. Soc*., 1997, **119**, 2497-2504.
24. M. Andratschke, K.-J. Range, C. Weigl, U. Schiessl, F.Z. Rau, and B. Naturforsch, *J. Chem. Sci*., 1994, **49**, 1282−1288.
25. H.Y. Ng, and W.T.A. Harrison, *Microporous and Mesoporous Mater*., 1998, **23**, 197-202.
26. P.F. Henry, and M.T. Weller, *Chem. Comm*., 1998, 2723-2724.

27. B.M. Gatehouse, *Acta Crystallogr*. *C*, 1989, **45**, 1674.
28. C.A. Juillerat, V. Kocevski, T.M. Besmann, and H.-C. zur Loye, *Inorg*. *Chem*., 2019, **58**, 4099-4102.
29. H-X. Deng, J. Li, S-S. Li, J-B. Xia, A. Walsh, and S-H. Wei, *Appl*. *Phys*. *Lett*., 2010, **96**, 162508.

Table 1. Reagents and Reaction Conditions for (**1**) – (**4**).

Compound	Reagents	Flux	Temperature profile
(**1**)	1 mmol CoF_2 1 mmol SiO_2	1.85 g CsCl 1.36 g CsF	Heated at 600 °C/h to 900 °C, held for 12 h and slow cooled to 400 °C at 6 °C/h
(**2**)	1 mmol CoF_2 4 mmol GeO_2	3.15 g CsCl 2.31 g CsF	Heated at 300 °C/h to 850 °C, held for 24 h and slow cooled to 400 °C at 6 °C/h
(**3**)	1 mmol CoF_2 2 mmol GeO_2	1.85 g CsCl 1.36 g CsF	Heated at 300 °C/h to 850 °C, held for 24 h and slow cooled to 400 °C at 6 °C/h
(**4**)	0.1 g compound (**1**)	1 g $RbNO_3$	Heated at 600 °C/h to 350 °C, held for 16 h and shut off

Table 2. Crystallographic and Refinement Data for (**1**) – (**4**).

Compound	(**1**)	(**2**)	(**3**)	(**4**)
empirical formula	$CsCo_{0.50}Si_{1.50}O_4$	$Co_{0.69}Cs_{1.29}Ge_{1.81}O_5$	$Cs_2CoGe_4O_{10}$	$Cs_{0.86}Rb_{0.14}Co_{0.50}Si_{1.50}O_4$
crystal color and habit	blue plate	deep blue irregular	deep blue block	blue block
F.W (g/mol)	268.51	423.02	775.13	261.73
crystal system	monoclinic	tetragonal	tetragonal	monoclinic
space group	*Im*	*I*-4	*I*-4	*Im*
a (Å)	8.9926(4)	7.4239(14)	7.3540(6)	8.996(2)
b (Å)	5.4599(2)	13.169(3)	13.112(1)	5.4500(10)
c (Å)	9.3958(6)	13.169(3)	13.112(1)	9.381(2)
β (°)	91.5928(18)	90	90	90.709(17)
Z	4	4	2	4
V (Å^3)	461.14(4)	725.8(3)	709.13(13)	459.89(17)
$\rho_{calc.}$ (mg/m^3)	3.868	3.871	3.630	3.780
crystal size (mm^3)	0.06x0.03x0.02	0.20x0.14x0.10	0.16x0.12x0.10	0.10x0.08x0.07
Flack parameter	0.50(7)	0.046(7)	0.013(7)	[a]
Goodness-of-fit on F^2	1.150	1.062	1.221	1.091
final *R* indices [I>2sigma(I)]	$R_1 = 0.0209$	$R_1 = 0.0206$	$R_1 = 0.0235$	$R_1 = 0.0309$
final *R* indices (all data)	$wR_2 = 0.0428$	$wR_2 = 0.0514$	$wR_2 = 0.0661$	$wR_2 = 0.0741$
largest diff. peak and hole (e/A^{-3})	0.757/-0.556	0.460/-0.368	0.712/-0.372	1.727/-1.126

[a] Twinning involves inversion, so Flack parameter cannot be determined.

Table 3. Selected Interatomic Distances (Å) for (**1**). *M*(1) and *M*(2) = 50/50 Co/Si.

	Exp.	**DFT**		**Error**
M(1) – O(2) x (2)	1.821(16)	1.9299	Co-O	
M(1) – O(3)	1.893(10)	1.9540	Co-O	
M(1) – O(5)	2.012(11)	1.9551	Co-O	
M(2) – O(5)	1.405(10)	1.5833	Si-O	
M(2) – O(6)	1.707(10)	1.6271	Si-O	
M(2) – O(1) x (2)	1.781(17)	1.6684	Si-O	
Si(1) – O(3)	1.550(10)	1.5865		2.35%
Si(1) – O(1) x (2)	1.572(17)	1.6015		1.88%
Si(1) – O(4)	1.680(12)	1.6720		-0.48%
Si(2) – O(4)	1.592(11)	1.6433		3.2%
Si(2) – O(2) x (2)	1.630(16)	1.6593		1.80%
Si(2) – O(6)	1.670(11)	1.6695		-0.03%

Table 4. Selected Interatomic Distances (Å) for (**2**). *M*(1) = Ge(1)/Co(1A) = 0.867/0.133 and *M*(2) = Co(1)/Ge(1A) = 0.85(4)/0.15(4).

M(1) – O(2)	1.723(4)
M(1) – O(1)	1.755(4)
M(1) – O(3)	1.760(3)
M(1) – O(1)	1.761(4)
M(2) – O(2) x (4)	1.926(4)

Table 5. Selected Interatomic Distances (Å) for (**3**).

	Exp.	**DFT**	**Error**
Co(1) – O(2) x (4)	1.948(4)	1.9796	1.62%
Ge(1) – O(1)	1.742(4)	1.7813	2.25%
Ge(1) – O(1)	1.762(3)	1.8035	2.35%
Ge(1) – O(2)	1.706(4)	1.7216	0.91%
Ge(2) – O(3)	1.760(3)	1.7954	2.01%

Table 6. Selected Interatomic Distances (Å) for (**4**). *M*(1) and *M*(2) = 50/50 Co/Si.

M(1) – O(2) x (2)	1.88(2)
M(1) – O(3)	1.897(17)
M(1) – O(5)	1.98(2)
M(2) – O(5)	1.38(2)
M(2) – O(6)	1.722(17)
M(2) – O(1) x (2)	1.70(2)
Si(1) – O(3)	1.532(18)
Si(1) – O(1) x (2)	1.63(2)
Si(1) – O(4)	1.68(2)
Si(2) – O(4)	1.60(2)
Si(2) – O(2) x (2)	1.59(2)
Si(2) – O(6)	1.67(2)

Table 7. DFT Calculated Crystallographic Data for (**1**) and (**3**).

	State	V (Å^3)	a (Å)	b (Å)	c (Å)	β (^{o})
(**1**)	FM	453.40	8.8325	5.4023	9.5050	91.3957
	AFM	451.58	8.8036	5.3878	9.5226	91.1401
(**3**)	FM	661.58	7.2156	7.2156	12.7067	90
	AFM	661.31	7.2150	7.2150	12.7038	90

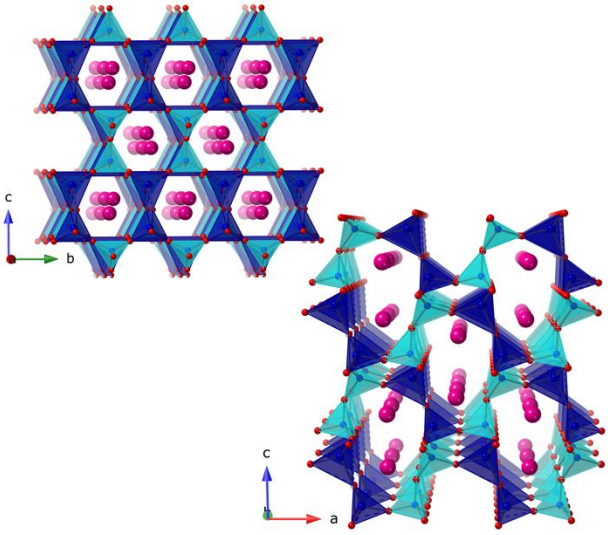

Figure 1. Crystal structure of (**1**) featuring hexagonal (six-membered) channels down the *a*-axis (top) and eight-sided cavities down the *b*-axis (bottom). The mixed (50/50) Co/Si sites are shown in deep blue while pure Si sites are shown in turquoise. Cs and O are depicted as pink and red spheres, respectively.

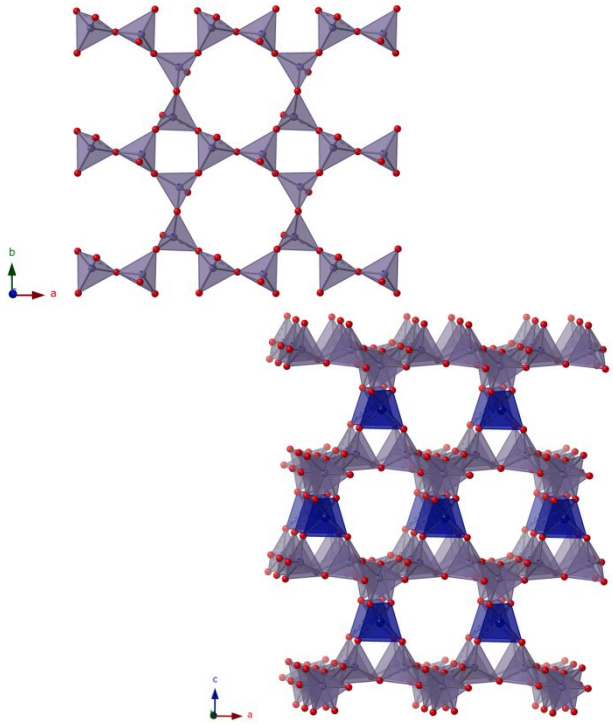

Figure 2. Illustration of the two-dimensional GeO_4 anionic sheet down the *c*-axis (top) in (**3**); assembly of the two-dimensional sheets into a three-dimensional cobaltogermanate framework (bottom). Ge and Co sites are shown in lavender and deep blue, respectively. Oxygen is shown in red.

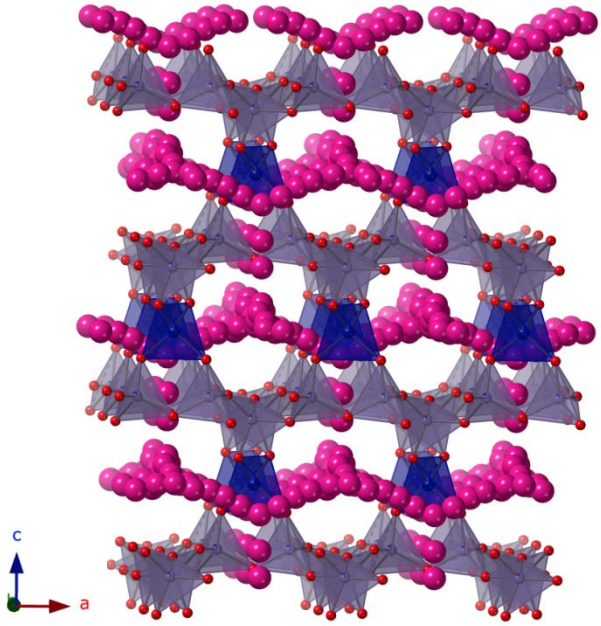

Figure 3. Polyhedral representation of (**3**). Ge and Co sites are shown in lavender and deep blue, respectively. Oxygen is shown in red. Cs is shown in pink.

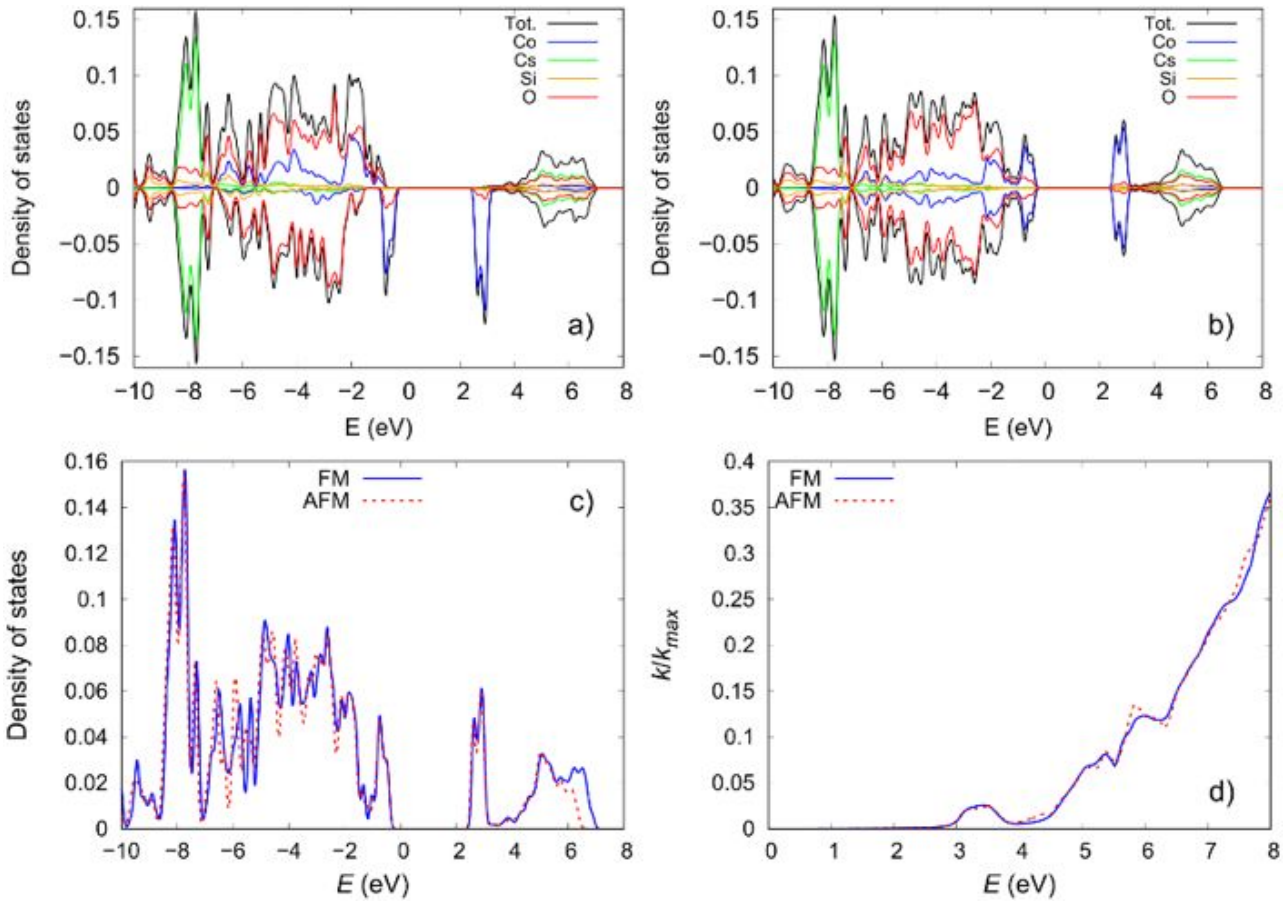

Figure 4. Projected density of states (PDOS) of (**1**) in: a) ferromagnetic (FM), and b) antiferromagnetic (AFM) state of $Cs(Co_{0.5}Si_{0.5})SiO_4$. The total DOS, Co, Cs, Si and O PDOS are shown in black, blue, green, orange and red, respectively. c) total DOS and d) absorption indexes of $Cs(Co_{0.5}Si_{0.5})SiO_4$ in FM and AFM state, shown in blue and red, respectively.

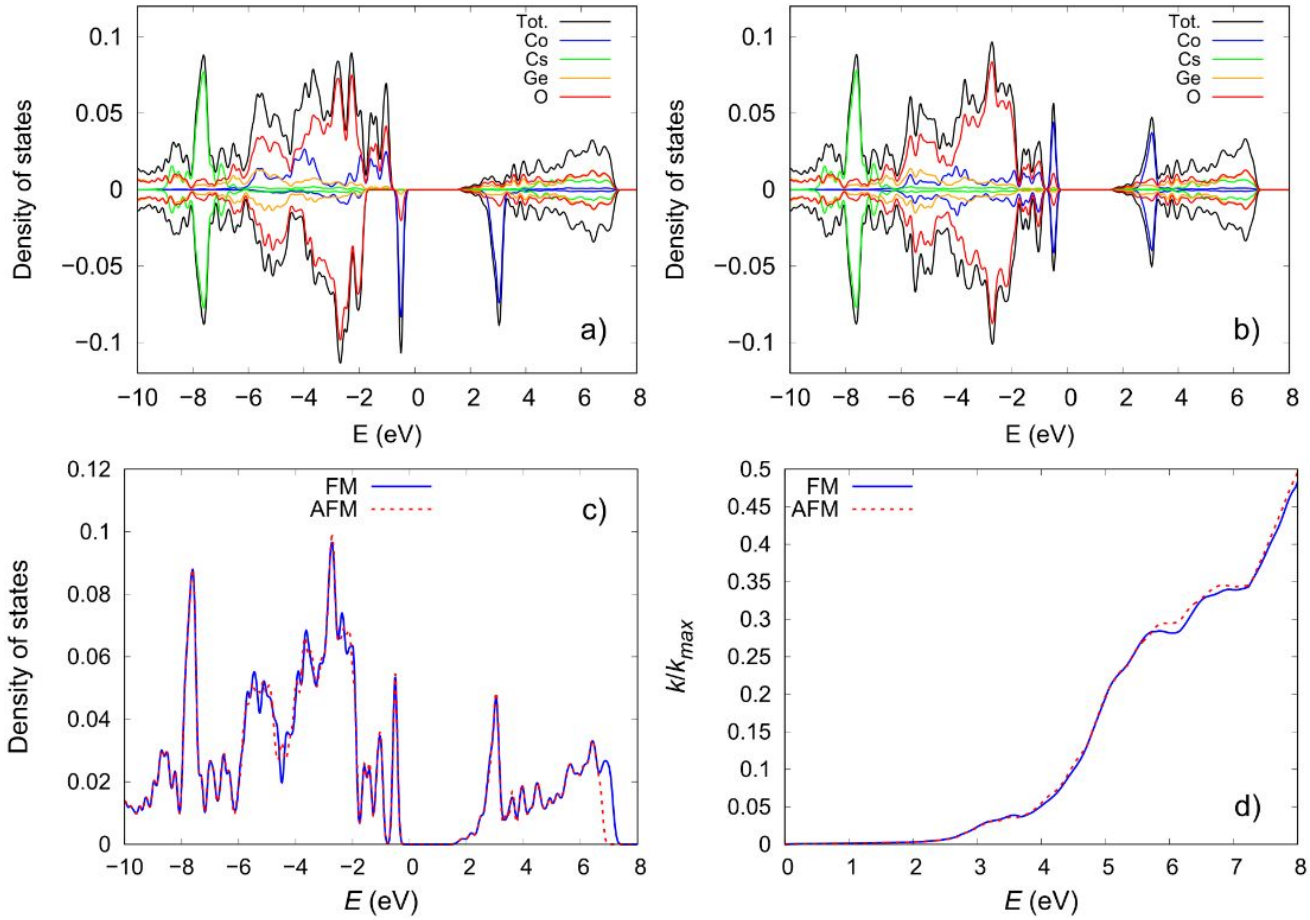

Figure 5. Projected density of states (PDOS) of (**3**) in: a) ferromagnetic (FM), and b) antiferromagnetic (AFM) state of $Cs_2CoGe_4O_{10}$. The total DOS, Co, Cs, Ge and O PDOS are shown in black, blue, green, orange and red, respectively. c) total DOS and d) absorption indexes of $Cs_2CoGe_4O_{10}$ in FM and AFM state, shown in blue and red, respectively.

Complex Cobalt Silicates and Germanates Crystallizing in a Porous Three-Dimensional Framework Structure

Mohammad Usman,[1] Mark D. Smith,[1] Vancho Kocevski,[2] Theodore Besmann,[2] and Hans-Conrad zur Loye,[1*]

[1]*Department of Chemistry and Biochemistry, University of South Carolina, Columbia, South Carolina 29208, United States*

[2]*Department of Mechanical Engineering, University of South Carolina, Columbia, South Carolina 29208, United States*

**Corresponding Author's Email: zurloye@mailbox.sc.edu*

Table of Contents Only Abstract

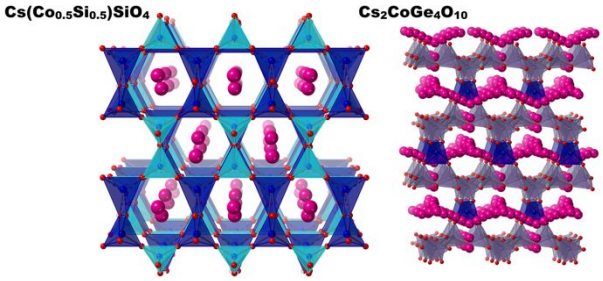

Single crystals of new cesium cobalt silicates and germanates exhibiting three-dimensional, ion-exchangeable crystal structures were grown from a mixed CsCl-CsF flux, and their electronic and magnetic properties studied using first-principles calculations.